

Giant vesicles at the prolate–oblate transition: A macroscopic bistable system

Hans-Günther Döbereiner * † and *Udo Seifert* *

*Max-Planck-Institut für Kolloid- und Grenzflächenforschung,
Kantstraße 55, 14513 Teltow-Seehof, Germany

†Department of Physics, University of British Columbia,
6224 Agriculture Road, Vancouver, British Columbia, Canada V6T 2A6

Abstract

Giant phospholipid vesicles are shown to exhibit thermally activated transitions between a prolate and an oblate shape on a time scale of several seconds. From the fluctuating contour of such a vesicle we extract ellipticity as an effective reaction coordinate whose temporal probability distribution is bimodal. We then reconstruct the effective potential from which we derive an activation energy of the order of $k_B T$ in agreement with theoretical calculations. The dynamics of this transition is well described within a Kramers model of overdamped diffusion in a bistable potential. Thus, this system can serve as a model for macroscopic bistability.

PACS: 05.40+j, 68.15+e, 82.70-y.

Macroscopic bistable systems for which thermal energy is sufficient to overcome the barrier in observable times are rare, quite in contrast to microscopic bistability so ubiquitous in nature [1]. In this paper, we consider bistability in the shape space of giant ($10\mu m$) phospholipid vesicles [2]. The shapes of these vesicles are determined by the minima of the bending energy of the vesicle membrane subject to constraints on the total area and enclosed volume [3, 4, 5]. A cut of the energy landscape along a path connecting nearby local minima then defines an effective double well potential in shape space. Since this potential is created by the vesicle due to its bending elasticity, our system is qualitatively different from the most prominent example of macroscopic bistability studied so far which is a one micron silica bead caught in a double well potential generated by an optical trap [6]. In the latter system, the (optical) potential is created externally in real space via gradients of the electromagnetic field.

A vesicle (shape) is not a static entity but shows thermally excited fluctuations, which are clearly visible by video microscopy, due to the softness of the vesicle membrane. At constant external parameters such as temperature, these fluctuations occur around a well-defined mean shape corresponding to the global minimum of bending energy. As temperature changes, these mean shapes usually evolve smoothly except at phase boundaries denoting so-called discontinuous transitions along which shapes of different symmetry have the same energy. In this report, we discuss the observation of vesicles at the prolate-oblate transition [7, 8]. These vesicles exhibit thermally activated jumps between the two states at constant external parameters. In Fig. 1, we show the contours of a typical sequence of vesicle shapes at equidistant times (6.3 s). A vesicle is seen to change its shape from a prolate with the mean symmetry axis within the focal plane to an oblate with the mean symmetry axis perpendicular to the focal plane and vice versa [9].

For a quantitative analysis, the contours of the vesicles in the focal plane are determined by image analysis [10, 11, 12]. We describe the shapes using polar coordinates,

$$r(\phi) = r_0 \left(1 + \sum_{n \geq 2} a_n \cos(n\phi) + \sum_{n \geq 2} b_n \sin(n\phi) \right), \quad (1)$$

where $a_1 = b_1 = 0$ implies the definition of the center of gravity of each contour as the origin. Since gravity holds the vesicles on the bottom of the

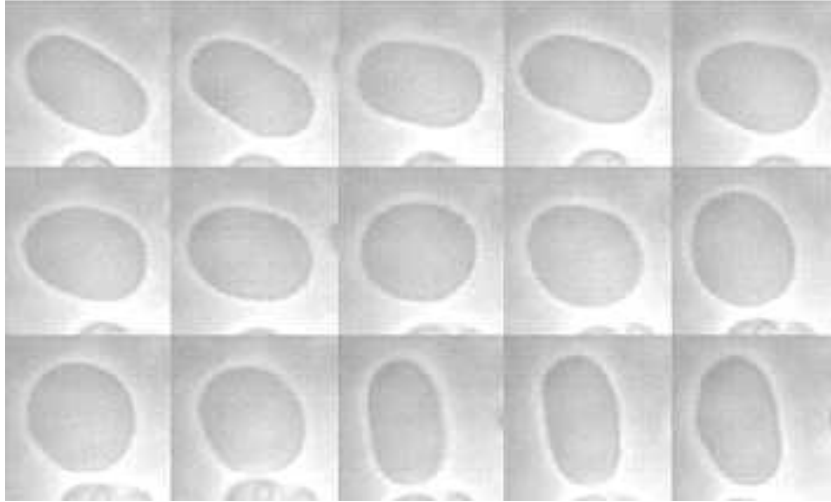


Figure 1: Prolate-oblate fluctuations of a DMPC vesicle. The snapshots are taken at equidistant time intervals of $\Delta t = 6.3$ s. The vesicle is seen to change its shape from a prolate with the mean symmetry axis within the focal plane to an oblate with the mean symmetry axis perpendicular to the focal plane and vice versa. Vesicles were prepared from stearyl-oleoyl-phosphatidylcholine (SOPC) or dimyristoyl-phosphatidylcholine (DMPC) in sucrose solution (50 mOsm) and incubated in excess glucose solution (48 mOsm). They were observed by video phase-contrast microscopy in a microchamber at constant temperature. Due to the slightly higher density of sucrose, the vesicle sink to the bottom of the observation chamber and rest gently against the glass wall. Thus, the free rotational diffusion of vesicle shapes is restricted to the 2 dimensions of the focal plane of the microscope. This stabilisation procedure is crucial for recording time series of vesicle shapes. Suitable vesicles were selected and observed near the boundary between the prolate and the oblate phase.

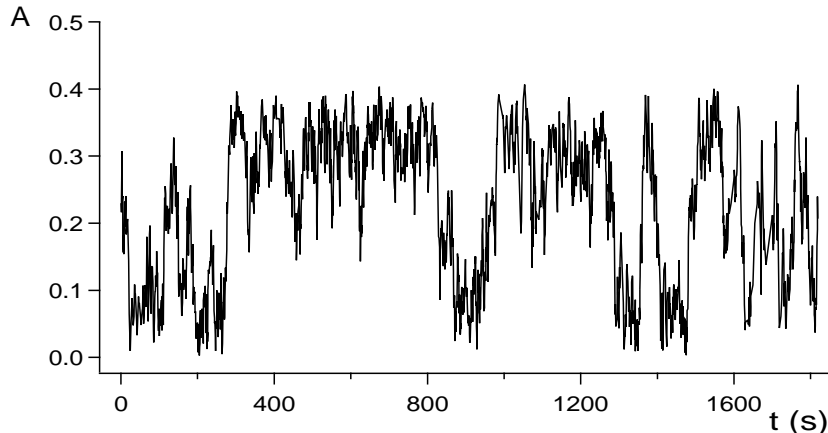


Figure 2: Time series of vesicle ellipticity $A = \sqrt{a_2^2 + b_2^2}$ near the prolate oblate transition. The ellipticity exhibits fluctuations around two distinct mean values which correspond to the prolate and oblate shape respectively. The shapes are quantified by extracting the vesicle contour via image analysis. Briefly, a contour point is defined by the gradient of the phase contrast profile across the membrane with respect to the local background level. Thereby, one finds a closed loop made up of points with sub-pixel resolution. The amplitudes a_2 and b_2 are then obtained from this contour via Eq. (1).

chamber, oblate shapes have a circular contour while prolate shapes (with their major axes parallel to the bottom) look ellipsoidal [13]. Thus, it is sufficient to monitor the amplitude $A \equiv \sqrt{(a_2^2 + b_2^2)} > 0$, which effectively measures the ellipticity of the vesicle contours.

In Fig. 2, a time series of A for a typical vesicle is shown. The apparent jumps in A between a small numerical value near zero and a larger positive number reflect the bistable nature of the system, already evident in Fig. 1. The larger values correspond to the fluctuating prolate shape, whereas the small values parallel the oblate vesicle with its fluctuating equatorial circular contour.

The diffusion in shape space is evident in Fig. 3, where we show the distribution of (a_2, b_2) . The points cluster at the center (the oblate phase) and along a circle (the prolates) because of the rotational symmetry of the

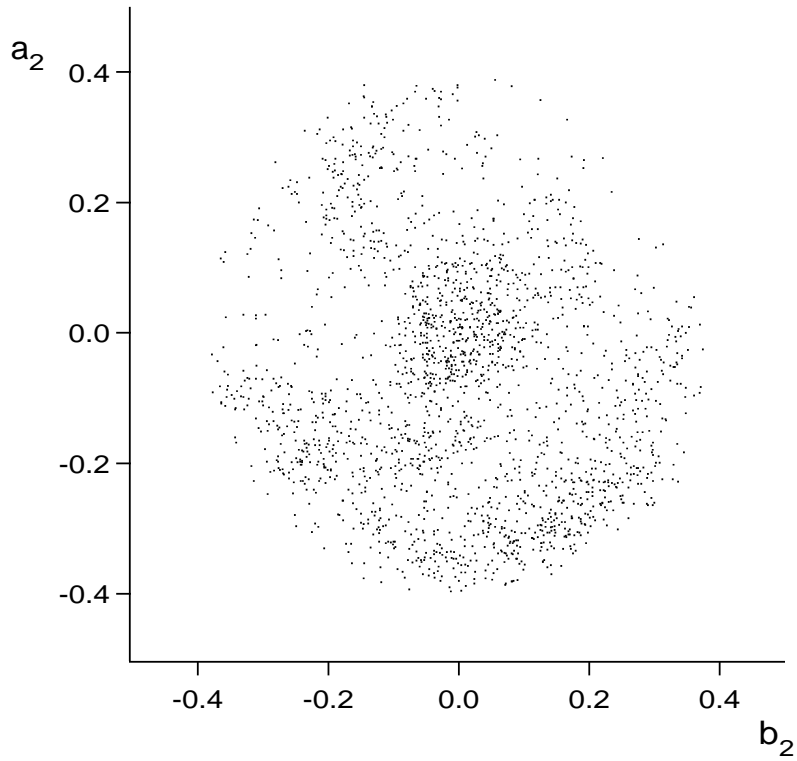


Figure 3: Distribution of instantaneous contour parameters (a_2, b_2) in a polar diagram. The dark center corresponds to the oblate shape, the darker rim to the prolate phase. Since the activation energy is of the order of $k_B T$, there is significant population also along the saddle points.

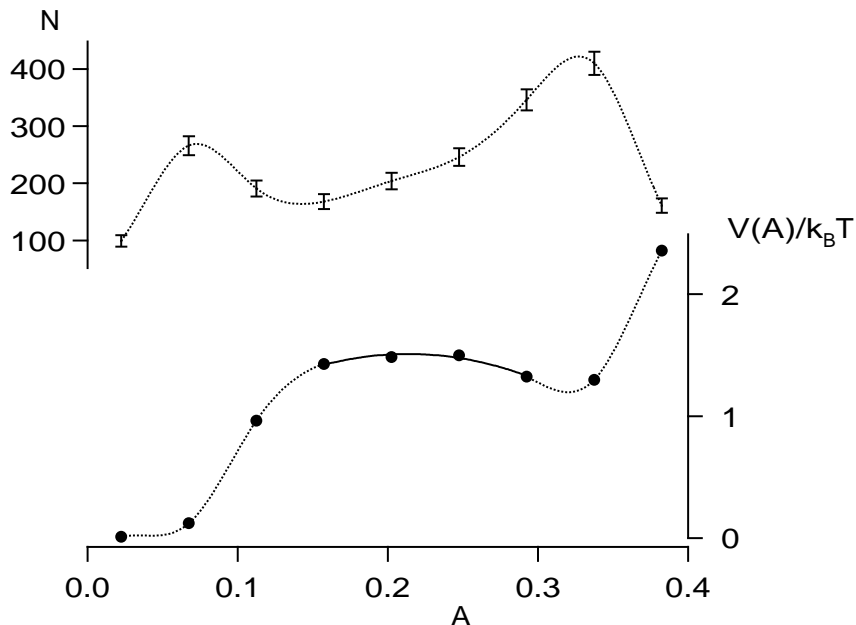


Figure 4: Histogram of events A of the ellipticity obtained with a bin size 0.045. The dotted lines are guides to the eye. The double well potential $V(A)$ is then reconstructed by using Eq. (2). The saddle point location at $A_s = 0.21$ and its curvature $w_s^2 = 29 k_B T$ are obtained via a fit (solid line) of the saddle to a parabola.

problem.

We now construct an effective potential for the variable A from the measured probability distribution $P(A)$, represented by a histogram of A as shown in Fig. 4. The probability to find the shape in the interval $[A, A + dA]$ (and any orientation α) is proportional to $dA A e^{-V(A)/k_B T}$, where $V(A)$ is an effective potential. The additional factor A arises from changing from cartesian coordinates a_2, b_2 to polar coordinates A and α . From the measured $P(A)$, we thus get

$$V(A)/k_B T = \ln A - \ln P(A) + \text{const} \quad (2)$$

as shown in Fig. 4. The activation energies $Q_{ob,pro}$ from the oblate and the prolate phase, respectively, thus obtained, are $Q_{ob} \simeq 1.5 \pm 0.1 k_B T$ and $Q_{pro} \simeq 0.2 \pm 0.1 k_B T$.

Although the prolate shape is metastable with a small barrier height Q_{pro} , it is nevertheless populated with a higher probability than the oblate minimum (compare Fig. 2). This is due to the measure factor AdA for the probability distribution $P(A)$, which reflects the larger density of states (with energy $V(A)$) of the prolate compared to the oblate shapes. All prolate vesicles with a fixed ellipticity A but varying orientation α have the same energy $V(A)$, while the oblates lack this orientational degree of freedom.

This observation of a vesicle as fluctuating in a bistable potential [14] is qualitatively different from the three other fluctuation effects observed in vesicles so far. (i) Fluctuations of quasispherical vesicles have long been used to extract the bending rigidity of bilayer membranes [10, 11, 15, 16]. Our experiment shows that this technique must fail if the available excess area of the vesicles is so large that the discontinuous character of the prolate-oblate transition becomes relevant. (ii) The budding transition [15, 17, 18], where a small satellite is expelled from a parent vesicle, is a strong first-order transition for which the activation energy cannot be surmounted thermally. One then observes pronounced fluctuations as the spinodal is approached [12]. (iii) Conformal diffusion of vesicles of higher topology involves diffusion along a one parameter continuous curve in a “flat” potential [19, 20].

A quantitative comparison of our experimental results with theoretical first-principle calculations is delicate. First, the presence of gravity makes even a calculation of the shape of lowest energy non-trivial [13]. However, since we expect gravity to be a minor correction of the energy, one can, in a first approximation, compare with the energy of free vesicles. Ignoring all shape fluctuations, this energy has been calculated for the two local minima (prolate and oblate) as well as for the intermediate stationary saddle point which is a non-axisymmetric ellipsoid [7, 8]. One finds a weak first-order transition with a maximal energy barrier between prolate and oblate for reasonable material parameters of the order $Q_{ob,pro}^0 \simeq 1 k_B T$. In principle, this energy barrier acquires an additional entropic contribution from the available phase space for fluctuations orthogonal to the reaction co-ordinate A . While for axisymmetric shapes, these entropic corrections can be calculated, a calculation for the non-axisymmetric saddle shape is far beyond presently available techniques. Since the measured activation energies are in reasonable

agreement with the theoretical value, our results indicate that these entropic corrections do not differ strongly for the three stationary shapes involved.

The dynamical aspects of this transition can be modeled as an overdamped Kramers escape problem in a potential $V(a_2, b_2) = V(A)$ [21, 22]. The diffusion in the angle co-ordinate can be integrated out, which leads to an one-dimensional diffusion process for the variable A in the effective potential $V_{\text{eff}}(A) \equiv V(A) - k_B T \ln A$. The corresponding Langevin equation reads $\gamma \partial_t A = -\partial V_{\text{eff}}/\partial A + \zeta$, where ζ is a stochastic force with the usual correlations $\langle \zeta(t)\zeta(t') \rangle = 2k_B T \gamma \delta(t - t')$. The effective friction coefficient γ is assumed to be independent of the shape and given by $\gamma = \text{const } \eta R^3$, where η is the viscosity of water and R the apparent radius of the oblate. The Kramers mean escape time from the oblate minimum becomes [22]

$$\tau_{ob} = \frac{\gamma \sqrt{2\pi k_B T}}{\omega_{ob}^2 \omega_s A_s} \exp Q_{ob}/T, \quad (3)$$

where the frequencies $\omega_{ob,s}$ are defined by a quadratic approximation to the energy in the oblate ($V(A) \approx V(0) + \frac{\omega_{ob}^2}{2} A^2$) and at the saddle at A_s ($V(A) \approx V(A_s) - \frac{\omega_s^2}{2} (A - A_s)^2$).

The pre-exponential factor in (3) becomes more transparent if it is expressed as $t_{ob} \sqrt{2\pi k_B T} / \omega_s A_s$ in terms of measurable quantities. Here, $t_{ob} \equiv \gamma / \omega_{ob}^2$ is the relaxation time for a_2 or b_2 fluctuations in the oblate phase. The measured dynamical correlation functions $\langle a_2(t)a_2(0) \rangle$ and $\langle b_2(t)b_2(0) \rangle$ can both be fitted against simple relaxational behavior with a decay time $t_{ob} \simeq 5 \pm 2$ s. Using the measured values $Q_{ob}/k_B T \simeq 1.5$, $A_s \simeq 0.21$ and $\omega_s^2 \simeq 29 k_B T$ as extracted from the potential (see Fig. 4), we obtain $\tau_{ob} \simeq 50 \pm 25$ s. This value is in reasonable agreement with the mean residence time $\bar{\tau}_{ob} \simeq 76 \pm 8$ s in the oblate phase as extracted directly from the time series $A(t)$ as shown in Fig. 2.

We now turn to a discussion of the prolate phase. For the fluctuations of the ellipticity A around its mean value $\langle A \rangle$, we find a relaxation time $\tau_A \simeq 8 \pm 1$ s. Fluctuations in α amount to rotational diffusion. For the latter, we find a rotational diffusion coefficient $D = (5.7 \pm 0.2) \times 10^{-3}$ rad²/s. It is this free diffusion which is responsible for the relative stability of the metastable prolate state. The mean escape time from the prolate phase should not be written in a Kramers form since the implicit assumption of Kramers theory that the activation energy is larger than $k_B T$ is violated on the prolate side.

To summarize, we have reported the observation of a macroscopic bistable system as evidenced by large shape fluctuations of giant vesicles between a prolate and oblate state. This result confirms the theoretical prediction of a weak discontinuous transition between prolate and oblate shapes. The mean escape time out of the metastable oblate state was found to be in reasonable agreement with the value obtained within a Kramers approach for the effective radial potential. Thus, fluctuating vesicle shapes may serve as a model system for further studies of macroscopically slow diffusion processes in a bistable potential.

We are grateful for discussions with E. Evans, M. Jarić, M. Kraus, R. Lipowsky, and M. Wortis.

References

- [1] P. Hänggi, P. Talkner, and M. Borkovec, *Rev. Mod. Phys.* **62**, 251 (1990).
- [2] R. Lipowsky, *Nature* **349**, 475 (1991); U. Seifert, *Adv. Phys.*, in press.
- [3] P. B. Canham, *J. Theoret. Biol.* **26**, 61 (1970).
- [4] W. Helfrich, *Z. Naturforsch.* **28c**, 693 (1973).
- [5] E. Evans, *Biophys. J.* **14**, 923 (1974).
- [6] A. Simon and A. Libchaber, *Phys. Rev. Lett.* **68**, 3375 (1992).
- [7] V. Heinrich, S. Svetina, and B. Žekš, *Phys. Rev. E* **48**, 3112 (1993).
- [8] M. Jarić, U. Seifert, W. Wintz, and M. Wortis, *Phys. Rev. E* **52**, 6623 (1995).
- [9] For a prolate shape, the mean symmetry axis is its major axis, whereas for an oblate shape, the mean symmetry axis coincides with the minor axis.
- [10] J. F. Faucon, M.D. Mitov, P. Méléard, I. Bivas, and P. Bothorel, *J. Phys. France* **50**, 2389 (1989).

- [11] H. P. Duwe, J. Käs, and E. Sackmann, *J. Phys. France* **51**, 945 (1990).
- [12] H.-G. Döbereiner, E. Evans, U. Seifert, and M. Wortis, *Phys. Rev. Lett.* **75**, 3360 (1995).
- [13] M. Kraus, U. Seifert, and R. Lipowsky, *Europhys. Lett.* **32**, 431 (1995).
- [14] We use the term “bistable” even though one of the locally stable shapes, the prolate, has a trivial one-fold degeneracy due to its orientational degree of freedom.
- [15] E. Evans and W. Rawicz, *Phys. Rev. Lett.* **64**, 2094 (1990).
- [16] G. Niggemann, M. Kummrow, and W. Helfrich, *J. Phys. II France* **5**, 413 (1995).
- [17] J. Käs and E. Sackmann, *Biophys. J.* **60**, 825 (1991).
- [18] L. Miao, U. Seifert, M. Wortis, and H. G. Döbereiner, *Phys. Rev. E* **49**, 5389 (1994).
- [19] F. Jülicher, U. Seifert, and R. Lipowsky, *Phys. Rev. Lett.* **71**, 452 (1993).
- [20] X. Michalet and D. Bensimon, *Science* **269**, 666 (1995).
- [21] H. Kramers, *Physica (Utrecht)* **7**, 284 (1940).
- [22] C. W. Gardiner, *Handbook of stochastic methods* , (Springer, Berlin 1994).